ISSN 1070-3284, Russian Journal of Coordination Chemistry, 2013, Vol. 39, No. 4, pp. 353–359. © Pleiades Publishing, Ltd., 2013.
Original Russian Text © G.A. Kostin, A.O. Borodin, N.V. Kurat'eva, E.Yu. Semitut, 2013, published in Koordinatsionnaya Khimiya, 2013, Vol. 39, No. 4, pp. 244–250.

Synthesis, Structures, and Thermolysis of New Heterometallic Cobalt, Nickel, and Copper Complexes with the $[Ru(NO)(NO_2)_4(OH)]^{2-}$ Anion as a Ligand

G. A. Kostin[a, b, *], A. O. Borodin[a], N. V. Kurat'eva[a, b], and E. Yu. Semitut[a]

[a] *Nikolaev Institute of Inorganic Chemistry, Siberian Branch, Russian Academy of Sciences, pr. akademika Lavrent'eva 3, Novosibirsk, 630090 Russia*

[b] *Novosibirsk State University, ul. Pirogova 2, Novosibirsk, 630090 Russia*

**e-mail: kostin@niic.nsc.ru*

Received October 8, 2012

Abstract—Heterometallic complexes with pyridine-N-oxide (PyO), $Ru(NO)(NO_2)_4(OH)Ni(PyO)_2(H_2O)] \cdot CH_3COCH_3$ (**I**), $[\{Ru(NO)(NO_2)_2(\mu\text{-}NO_2)_2(\mu\text{-}OH)Co\}_2(\mu\text{-}PyO)] \cdot H_2O \cdot CH_3COCH$ (**II**), and $[Ru(NO)(NO_2)_4(OH)Cu(PyO)_2]$ (**III**), are isolated in the reactions of $Na_2[Ru(NO)(NO_2)_4(OH)]$ with nitrates of the corresponding metals in the presence of the organic ligand. The compounds synthesized are characterized by IR spectra, thermal analysis, and X-ray diffraction analysis. Depending on the M^{2+} cation, the ruthenium cation is coordinated through the bidentate (**III,** Cu^{2+}) or tridentate (**I**, Ni^{2+} and **II**, Co^{2+}) mode involving the bridging OH group and one or two NO_2 groups. The thermal decomposition of complex **II** results in the formation of a $Co_{0.5}Ru_{0.5}$ solid solution, which is thermodynamically stable under the decomposition conditions. The thermolysis of complexes **I** and **III** in a hydrogen atmosphere leads to the formation of metastable solid solutions.

DOI: 10.1134/S1070328413040064

INTRODUCTION

One of promising directions of research in the area of the chemistry of ruthenium nitroso complexes is related to the development of catalytic technologies using supported powders of particles of different dispersity [1–3]. In this area, the use of catalysts based on solid solutions of ruthenium with cheaper metals makes it possible to decrease their cost and, in some cases, results in a synergetic increase in the catalytic activity [4]. The use of precursors already containing two different metals is rather promising for the synthesis of bimetallic catalysts. Comparatively low thermolysis temperatures for similar precursors in a reductive atmosphere allow one to obtain phases of individual metals and solid solutions, including metastable ones. The most part of studies in this area is devoted to binary complex salts of nitrosoaminoruthenium cations [5–7] in which the counterions containing different metals are bound by the electrostatic interaction only. At the same time, the synthesis of heterometallic complexes in which the nitrosoruthenium group is linked with the transition metal through the short bridging ligand (as, e.g., in cyanometallates [8–10]) enlarges the scope of objects that are potentially suitable as precursors.

We have earlier shown that the use of heterometallic cobalt complexes as bimetallic precursors [11] gives a stable Ru–Co solid solution in which the metal ratio is determined by the stoichiometry of the initial complex. Since in the Ru–Ni and Ru–Cu systems the mutual solubility of metals in the solid state is restricted or absent, it is of interest to synthesize heterometallic complexes of these metals and to study their thermal properties for the formation of metastable solid solutions. The studies of the thermolysis of the $[Ru(NO)(NO_2)_4(OH)NiPy_3]$ complex [11] showed that the thermal decomposition in an inert atmosphere led to the formation of solid solutions, whose composition was close to the solubility boundaries of these metals.

In this work, the heterometallic complexes of copper, nickel, and cobalt with $[Ru(NO)(NO_2)_4(OH)]^{2-}$ and pyridine-N-oxide as ligands were synthesized and studied by X-ray diffraction analysis. Their thermolysis products in inert and reductive atmospheres were examined.

EXPERIMENTAL

All reagents and solvents used were at least reagent grade, and $Na_2[Ru(NO)(NO_2)_4(OH)] \cdot 2H_2O$ was synthesized from ruthenium(III) chloride according to a described procedure [12].

Synthesis of $[Ru(NO)(NO [Ru(NO)(NO_2)_2(\mu\text{-}NO_2)_2(\mu\text{-}OH)Ni(PyO)_2(H_2O)] \cdot CH_3COCH_3$ (I). Weighed samples of $Ni(NO_3)_2 \cdot 6H_2O$ (0.1485 g, 5.1×10^{-4} mol) and $Na_2[Ru(NO)(NO_2)_4(OH)] \cdot 2H_2O$ (0.2111 g, 5.1×10^{-4} mol) were dissolved in acetone

(6 mL), and the mixture was stirred for 1 h. A precipitate of $NaNO_3$ was separated, a solution of pyridine-N-oxide (1.04 mL) in acetone (0.67 mol/L) was added to a transparent yellow-green solution, and the resulting solution was stirred for 30 min. Diethyl ether (6 mL) was added to the mixture cooled to −5°C, and complex **I** was isolated as a solvate with acetone. The yield of complex **I** was 87%.

For $C_{13}H_{19}N_7O_{14}NiRu$			
calculated (%):	C, 23.73;	H, 2.89;	N, 14.91.
Found (%):	C, 23.24;	H, 2.61;	N, 15.35.

IR (ν, cm^{-1}): 3460 ν(OH); 1907 ν(NO) of nitroso group; 1465, 1436 $\nu_{as}(NO_2)$; 1332, 1317 $\nu_s(NO_2)$; 1207 ν(NO) of pyridine oxide molecules; 821, 833 $\delta(NO_2)$.

Synthesis of [{RuNO(NO$_2$)$_2$(μ-NO$_2$)$_2$(μ-OH)Co}$_2$(μ-PyO)] · H$_2$O · CH$_3$COCH$_3$ (II). Weighed samples of $Co(NO_3)_2 \cdot 6H_2O$ (0.0582 g, 2.0×10^{-4} mol) and $Na_2[Ru(NO)(NO_2)_4(OH)] \cdot 2H_2O$ (0.0828 g, 2.0×10^{-4} mol) were dissolved in acetone (3 mL), and the mixture was stirred for 1 h. After a precipitate of sodium nitrate was separated, pyridine-N-oxide (0.057 g, 6×10^{-4} mol) was added to the obtained solution. The reaction mixture was stirred for 30 min and cooled to −5°C, diethyl ether (4 mL) was added, and complex **II** was isolated as dark red crystals. The yield of complex **II** was 84%.

For $C_{28}H_{35}N_{15}O_{27}Co_2Ru_2$			
calculated (%):	C, 25.27;	H, 2.63;	N, 15.80.
Found (%):	C, 25.83;	H, 2.51;	N, 16.32.

IR (ν, cm^{-1}): 3531, 3464 ν(OH); 1902 ν(NO) of nitroso group; 1444, 1402 $\nu_{as}(NO_2)$; 1338, 1319 $\nu_s(NO_2)$; 1205 ν(NO) of pyridine oxide molecules; 829 $\delta(NO_2)$.

Synthesis of [RuNO(NO$_2$)$_2$(μ-NO$_2$)$_2$(μ-OH)Cu(PyO)$_2$] (III). Weighed samples of $Cu(NO_3)_2 \cdot 3H_2O$ (0.12 g, 5×10^{-4} mol) and $Na_2[RuNO(NO_2)_4OH] \cdot 2H_2O$ (0.207 g, 5×10^{-4} mol) were dissolved in acetone (4 mL), and the mixture was stirred for 1 h. After a precipitate of sodium nitrate was separated, a solution of pyridine-N-oxide (1.5 mL) in acetone (0.67 mol/L) was added to the reaction mixture, which was stirred for 30 min more. The solution was cooled to −5°C, diethyl ether was added, and complex **III** was isolated as dark green crystals. The yield of complex **III** was 92%.

For $C_{10}H_{11}N_7O_{12}CuRu$			
calculated (%):	C, 20.51;	H, 1.88;	N, 16.75.
Found (%):	C, 19.90;	H, 2.04;	N, 16.20.

IR (ν, cm^{-1}): 3331 ν(OH); 1907 ν(NO) of nitroso group; 1467, 1444, 1392 $\nu_{as}(NO_2)$; 1344, 1328, 1313 $\nu_s(NO_2)$; 1207 ν(NO) of pyridine oxide molecules; 817, 837 $\delta(NO_2)$.

Thermal analysis was carried out on a Paulic-Erdey Q-1000 derivatograph in a helium atmosphere in open crucibles with the heating rate ranging from 1 to 10°C/min. Energy dispersive analysis was performed on a JEOL JSM 6700F scanning electron microscope with an EX23000BU(EDS) energy dispersive analyzer.

X-ray diffraction study was carried out on a DRON-SEIFERT-RM4 diffractometer (CuK_α radiation, graphite monochromator, reflected beam). Diffraction patterns were detected in the stepwise regime in the 2θ range from 5° to 60° for the complexes and from 5° to 135° for the thermolysis products. The compositions of solid solutions were estimated from the additivity of atomic volumes.

X-ray diffraction analysis. Single crystals of the complexes were obtained by the slow diffusion of hexane or diethyl ether into solutions of the complexes in acetone. Diffraction data were obtained on a Bruker Nonius X8Apex CCD diffractometer at 298 K (MoK_α radiation, graphite monochromator, φ, ω scan mode). Structures **I–III** were solved by direct methods and refined by the full-matrix least-squares method (SHELXTL) [13]. Positions of hydrogen atoms were calculated geometrically. The main crystallographic parameters and experimental characteristics are given in Table 1.

The coordinates of atoms and other parameters of structures **I–III** were deposited with the Cambridge Crystallographic Data Centre (nos. 902905 (**I**), 902906 (**II**), and 902907 (**III**); deposit@ccdc.cam.ac.uk or http://www.ccdc.cam.ac.uk/data_request/cif).

RESULTS AND DISCUSSION

As in the earlier synthesized complexes with triphenylphosphine oxide (TPPO) and pyridine [11, 14], in complexes **I–III** with pyridine oxide the ruthenium fragment acts as a bi- and tridentate ligand, coordinating to the M^{2+} cation by the bridging hydroxo and nitro groups. However, the formation of heterometallic complexes in the presence of pyridine-N-oxide has several specific features. First, this reaction is more sensitive to the ratio of the starting reagents. When a six- and sevenfold molar excess of pyridine-N-oxide is applied or $[M(PyO)_6](NO_3)_2$ are used as starting compounds, the major products are poorly soluble binary complex salts $[M(PyO)_6][RuNO(NO_2)_4OH]$, whose composition was confirmed by elemental analysis data. The quantitative formation of the heterometallic complexes with the coordination of the ruthenium anion to the non-ferrous metal cation is observed only at a two- and threefold molar excess of pyridine-N-oxide with respect to Ru–M. Second, in some cases, the coordination sphere of M^{2+} of the complexes with pyridine oxide includes water molecules. Third, in the

Table 1. Crystallographic data and experimental and refinement characteristics for structures **I**–**III**

Parameter	Value		
	I · CH_3COCH_3	**II** · H_2O · CH_3COCH_3	**III**
Empirical formula	$C_{13}H_{19}N_7O_{14}NiRu$	$C_{28}H_{35}N_{15}O_{27}Co_2Ru_2$	$C_{10}H_{11}N_7O_{12}CuRu$
Formula weight	657.13	1329.21	585.86
Crystal system	Monoclinic	Monoclinic	Orthorhombic
Space group	$P2_1$	$P2_1/n$	$Fdd2$
a, Å	12.3896(16)	10.3794(2)	32.8477(19)
b, Å	5.7463(5)	25.7258(7)	36.969(2)
c, Å	16.146(2)	18.4319(5)	6.3470(3)
α, deg			
β, deg	94.287(3)	95.827(1)	
γ, deg			
V, Å^3	1146.3(2)	4896.2(2)	7707.4(7)
Z	2	4	16
ρ_{calcd}, g/cm^3	1.904	1.803	2.016
μ, mm^{-1}	1.564	1.373	1.966
Crystal size, mm	0.35 × 0.08 × 0.04	0.33 × 0.22 × 0.07	0.22 × 0.04 × 0.02
F(000)	660	2654	4608
Scan range, θ, deg	1.65–28.28	1.36–26.37	2.20–26.37
Ranges of reflection indices	$-16 \le h \le 16$, $-4 \le k \le 7$, $-21 \le l \le 21$	$-12 \le h \le 7$, $-32 \le k \le 32$, $-22 \le l \le 23$	$-40 \le h \le 40$, $-46 \le k \le 46$, $-4 \le l \le 7$
Number of measured reflections	9111	31151	13745
Number of independent reflections (R_{int})	4297 (0.0392)	9951 (0.0295)	3205 (0.0403)
Number of reflections with $I \ge 2\sigma(I)$	3945	7782	2781
Number of refined parameters	329	709	281
Goodness-of-fit	1.061	1.081	1.048
R_1, wR_2 ($I > 2\sigma(I)$)	0.0498, 0.1202	0.0386, 0.0997	0.0335, 0.0810
R_1, wR_2 (all reflections)	0.0545, 0.1233	0.0549, 0.1071	0.0419, 0.0839
$\Delta\rho_{max}/\Delta\rho_{min}$, e Å^{-3}	1.936/–3.484	1.253/–0.844	0.495/–0.373

case of cobalt, a tetranuclear complex is formed, where one of the pyridine oxide molecules is bridging between two Ru–Co fragments.

The crystalline lattice of complex **I** is formed by molecular fragments $[Ru(NO)(NO_2)_4(OH)Ni(PyO)_2(H_2O)]$ (Fig. 1) joined by hydrogen bonds O(20)–H···O(2) (x, $y - 1$, z) and O(20)–H···O(2) ($1 - x$, $y - 1/2$, $1 - z$). The nickel cation is in the distorted octahedral environment of six oxygen atoms: two pyridine oxide molecules, one coordinated water molecule, and three bridging groups (OH, NO_2). The Ni–O distances were 2.011(4)–2.077(4) Å (Table 2). The central angles at the nickel atom range from 85.5(2)° to 95.8(2)°.

The crystalline lattice of complex **II** is formed by tetranuclear molecular particles $[[Ru(NO)(NO_2)_4(OH)Co(PyO)_2]_2$-μPyO]. Three oxygen atoms of the OH and NO_2 bridging groups and three oxygen atoms of molecules of the organic ligands are coordinated to the cobalt atom in each $[Ru(NO)(NO_2)_4(OH)Co(PyO)_2]$ fragment. As in the case of the heterometallic cobalt complexes with pyridine and TPPO, the Co–ONO bonds are by 0.15–0.2 Å longer than the Co–OH and Co–OPy distances. The tetramer is additionally stabilized by hydrogen bonds between the OH group of one $[Ru(NO)(NO_2)_4(OH)Co(PyO)_2]$ fragment and the oxygen atom of the nearest pyridine oxide molecule of the second fragment (Fig. 2).

The structure of the Ru–Cu coordination node in complex **III** (Fig. 3) is similar to that of the earlier synthesized $[Ru(NO)(NO_2)_4(OH)Cu(Py)_2]$ complex with the coordination mode 4 + 2 [15]. The shortest bonds are formed by the copper cation with the oxygen atoms of the pyridine oxide molecules (1.910(4) and 1.930(5) Å), the bridging hydroxo group (1.963(4) Å), and the bridging nitro group (2.025(4) Å). The dis-

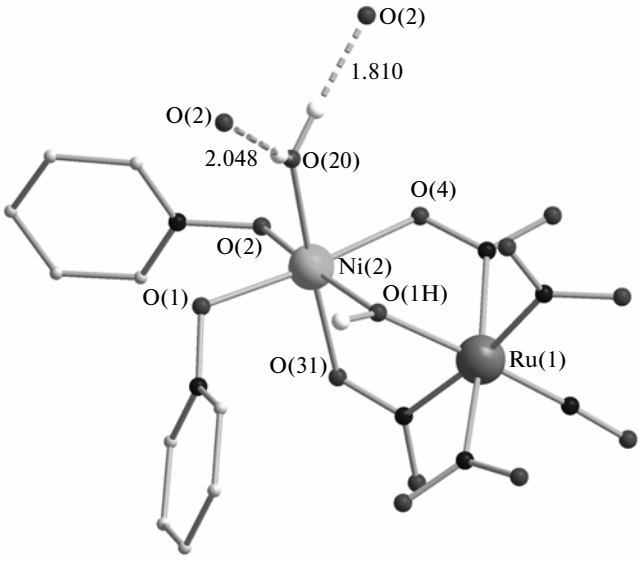

Fig. 1. Structure of complex **I**. Intermolecular hydrogen bonds are shown by dashed lines.

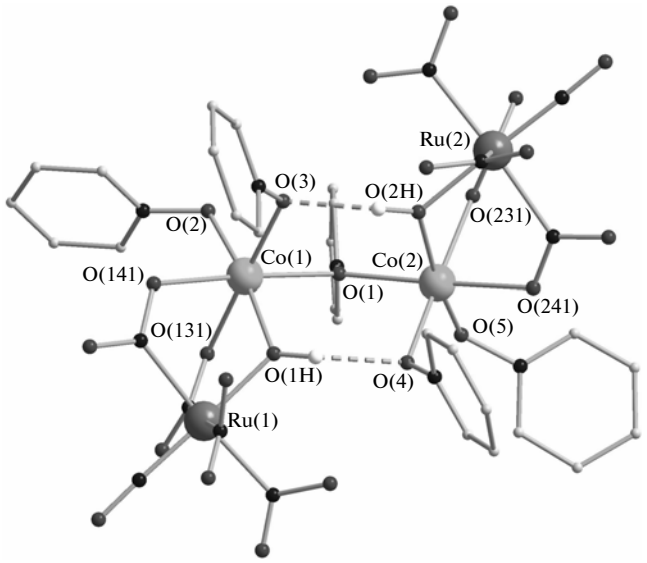

Fig. 2. Structure of complex **II**. Intramolecular hydrogen bonds are shown by dashed lines.

torted square environment (the bond angles at the copper atom vary in the range from 83.5° to 95.4°) is supplemented along the axial coordinate by the oxygen atoms of the nitro groups O(41) and O(42) (x, y, $z - 1$) (Cu–O 2.466(5) and 2.491(5) Å).

The structure of the ruthenium fragment changes weakly upon coordination. As for the earlier studied heterometallic complexes with this anion, some elongation of the N–O bonds in the bridging nitro groups is observed (Table 3).

The thermal decomposition curves for complexes **I–III** in a helium atmosphere are presented in Fig. 4. Four to five stages of decomposition can be distinguished from the curves of differential mass loss for all the three complexes. The temperatures of decomposition onset for complexes **II** (154°C) and **III** (136°C) are similar to those for the pyridine analogs [11]. Complex **I** is less stable because of the solvate acetone molecules and begins to lose its mass at 50–60°C, and the experimental mass loss at the first stage (below 95°C) equal to 4.8% is close to the theoretical value (4.3%) corresponding to the solvate acetone molecule. The study of the thermal decomposition of different $[Ru(NO)(NO_2)_4(OH)]$ salts [16, 17] shows that the first decomposition stage is associated with the detachment of the hydroxo group and the mass loss corresponding to this stage (40–50 au) corresponds to the removal of at least one nitro group. For complexes **II** and **III**, the first endothermic stage is finished at 180–190°C and the mass loss (based on one ruthenium atom) is 45–55 au, which is qualitatively consistent with the character of ruthenium anion decomposition. The nitrosoruthenium group decomposes in the temperature range from 200 to 400°C, which is accompanied in these complexes by the elimination of organic ligands and their oxidation by the nitroso and nitro groups.

Table 2. Characteristic distances in the coordination environment of the non-ferrous metal for complexes **I–III**

Bond	d, Å		
	I	**II**	**III**
M–OH	2.014(5)	2.007(3), 2.006(3)	1.963(4)
M–L	2.011(4)	1.995(4)–2.143(3)	1.910(4)
	2.079(4)		1.930(5)
M–ONO	2.063(5)	2.133(4)–2.196(4)	2.025(4)
	2.077(4)		2.466(5)
			2.491(5)
$M–OH_2$	2.054(5)		

The character of decomposition of the nickel and copper complexes in inert and reductive atmospheres (Fig. 4) is almost the same below 200–210°C, indirectly indicating the absence of redox processes at the first stages of decomposition. The further reduction of the nitrosoruthenium group in a hydrogen atmosphere is faster and forms metallic phases (including solid solutions) at 300–400°C.

The thermolysis products were identified by the powder diffraction method. Bimetallic mixtures are the only decomposition products observed in the diffraction patterns (Table 4). For the decomposition in a reductive atmosphere, the experimental mass loss corresponds well to the theoretical value for the metallic products. For the decomposition in an inert atmosphere, the theoretical mass loss corresponding to the "M–Ru" products is lower than the experimental value because of the presence of amorphous carbon,

which is formed due to the partial oxidation of the ligands, in the final products.

The Co–Ru system forms a continuous series of solid solutions. The diffraction pattern of the metallic powder obtained by the thermolysis of complex **II** exhibits peaks related to a $Ru_{0.5}Co_{0.5}$ solid solution corresponding to the stoichiometry of the starting complex, and the positions of the peaks coincide with the standard values for the $Ru_{0.50}Co_{0.50}$ solid solution (standard data file PDF, 65-8976 [18]). The average size of the crystallites determined by peak broadening is 30–40 nm. The Ni–Ru phase diagram is peritectic. At temperatures lower than the peritectic point (1550°C), only two types of solid solutions [19] are thermodynamically stable: those based on the face centered cubic (fcc) crystalline lattice of nickel and the crystalline lattice of ruthenium with the hexagonal close packing (hcp), respectively. The mutual solubility of these metals is 5–10% in the temperature range from 500 to 700°C. Solid residues obtained after the thermal decomposition of complex **I** in an inert atmosphere or in hydrogen are a mixture of two solid solutions based on nickel and ruthenium. A decrease in the final thermolysis temperature on going to the reductive atmosphere results in the enrichment of the ruthenium-based solid solution in nickel. Only one product, viz., a solid solution based on the hcp of ruthenium, can be identified by powder diffraction at temperatures below 450°C. Since the energy dispersive analysis data and the experimental mass loss under these conditions are well consistent with the formation of the 1 : 1 metallic mixture, it can be assumed that an X-ray amorphous nickel-based solid solution is the second product at the final temperature equal to 300–400°C as well.

No regions of mutual solubility of these metals in the solid state are observed in the phase diagram of the Ru–Cu system. Metallic copper and ruthenium are the only products of the thermolysis of complex **III** in an inert atmosphere at a final temperature of 850°C. A decrease in the decomposition temperature to 430°C on going to the reductive atmosphere results in the formation of two solid solutions based on copper and ruthenium. At a lower heating rate (1°C/min), the thermal decomposition of complex **III** ceases at 300–320°C, and the final mass loss corresponds well to the formation of a metallic mixture. As in the case of nickel complex **I**, a decrease in the decomposition temperature results in a decrease in the crystallite size and mutual enrichment of the solid solutions formed.

A comparison of the data on the thermal decomposition of complexes **I–III** in an atmosphere of helium and hydrogen and on the products obtained suggests that the decomposition stage in an inert atmosphere at 400–500°C observed for all complexes corresponds to the reduction of ruthenium oxide according to the equation

$$RuO_2 + 2C = Ru + 2CO,$$

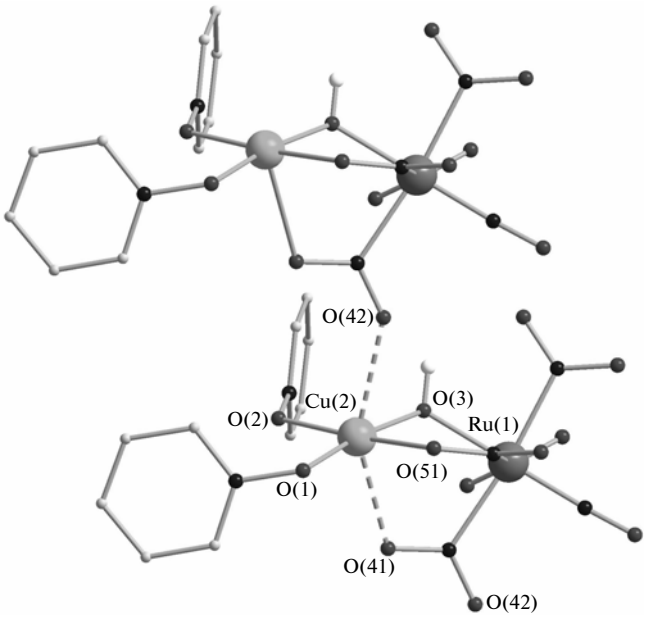

Fig. 3. Structures of two adjacent molecules of complex **III**. Additional copper–oxygen interactions are shown by dashed lines.

where carbon-containing thermolysis products of the organic ligands participate as reducing agents. Indeed, the mass loss at this stage (~10% of the initial mass for all compounds studied) coincides satisfactorily with

Table 3. Characteristic distances and bond angles in the coordination environment of ruthenium for complexes **I–III**

Bond	*d*, Å		
	I	**II**	**III**
Ru–NO	1.754(5)	1.754(4)	1.767(6)
		1.758(5)	
Ru–OH	1.964(4)	1.952(3)	1.960(4)
		1.952(3)	
$Ru–NO_{2\,term}$*	2.067	2.073	2.087
$N–O(NO_{2\,term})$*	1.238	1.209	1.225
Ru–μ-NO_2*	2.090	2.091	2.087
N–O(μ-NO_2)*	1.214	1.223	1.235
N–O(μ-NO_2) **	1.294	1.263	1.256
Angle	ω, deg		
	I	**II**	**III**
$ONO(NO_{2\,term})$*	120.1	118.3	120.9
ONO(μ-NO_2)*	117.8	118.7	118.8

Notes: * Average bond lengths and angles for the corresponding fragments.

** Distances to the oxygen atoms involved in coordination to M^{2+}.

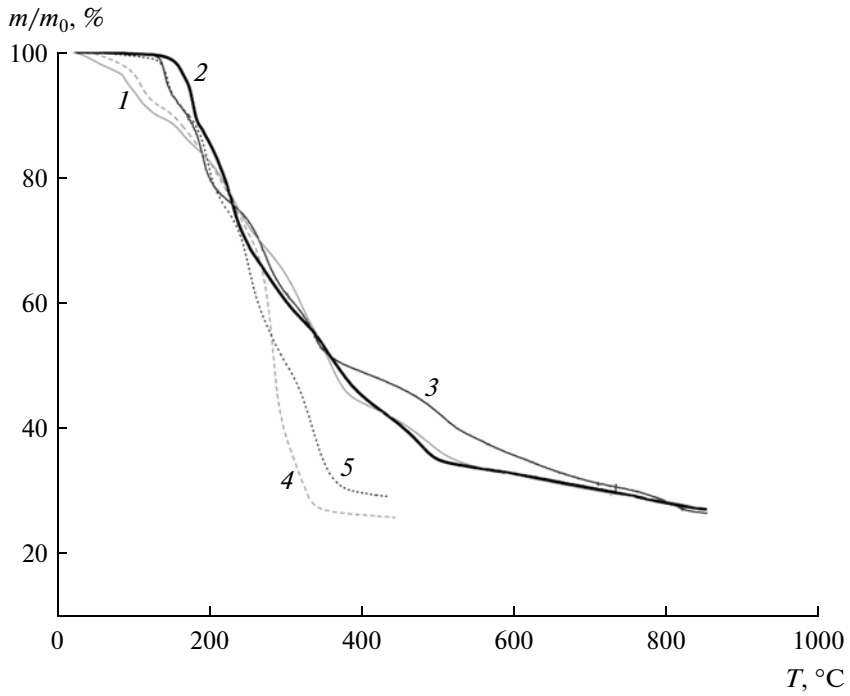

Fig. 4. Thermograms for complexes (*1*) **I**, (*2*) **II**, and (*3*) **III** in an inert (He) atmosphere and for complexes (*4*) **I** and (*5*) **III** in a reductive (H_2) atmosphere.

the theoretical value (10.0% for complex **III** and 8.9% for complexes **I** and **II**). Metallic copper is the single product of the decomposition of complex **III** in a helium atmosphere below 400°C. The subsequent keeping of the sample for 240 min at this temperature results in a mass loss of 10.5% of the initial value (Table 4). The final products contain metallic copper and ruthenium forming no solid solutions in this case, unlike the thermolysis products of complex **III** in hydrogen at the same temperature.

Table 4. Phase composition of the thermolysis products of complexes **I**–**III** upon calcination with a rate of 10°C/min

Complex	Atmosphere	Final temperature, °C	Final mass, %	Ratio M : Ru	Phases	Crystallite size, nm
I	He	860	27.2		$Ni_{0.9}Ru_{0.1}$ $Ni_{0.15}Ru_{0.85}$	35–40
	H_2	600	25.8		$Ni_{0.94}Ru_{0.06}$ $Ni_{0.26}Ru_{0.74}$	14–21
	H_2	450	24.6	1, 1 : 1	$Ni_{0.3}Ru_{0.7}$	6–8
	H_2*	400	24.4	1, 2 : 1	$Ni_{0.3}Ru_{0.7}$	3–5
	H_2*	300	24.7	1, 2 : 1	$Ni_{0.33}Ru_{0.67}$	3–5
II	He	860	28.4		$Co_{0.5}Ru_{0.5}$	32–36
III	He	860	29.5		Cu + Ru	42–49
	He	400	50.5		Cu	
	He	400 (240 min annealing)	39.9		Cu + Ru	
	H_2	450	29.1	1, 1 : 1	$Cu_{0.75}Ru_{0.25}$ $Cu_{0.05}Ru_{0.95}$	6–7
	H_2*	350	29.0	1, 2 : 1	$Cu_{0.84}Ru_{0.16}$ $Cu_{0.18}Ru_{0.82}$	4–6
	H_2*	300	28.9	1, 2 : 1	$Cu_{0.84}Ru_{0.16}$ $Cu_{0.3}Ru_{0.7}$	4–6

* The heating rate is 1°C/min.

Based on the above data, we assume that the decomposition of the complexes in a hydrogen atmosphere leads to the simultaneous reduction of a non-ferrous metal (Co, Ni, Cu) and ruthenium favoring the formation of solid solutions, whereas the decomposition in a helium atmosphere results in the formation of metallic ruthenium at 400–500°C due to the reduction of RuO_2 by the products of organic ligand decomposition, and the non-ferrous metal (Cu, Ni, Co) is reduced at lower temperatures.

ACKNOWLEDGMENTS

This work was supported by the Federal target program "Scientific and Scientific–Pedagogical Personnel of Innovative Russia" for 2009–2013 (agreement 14.V37.21.0141) and the Russian Foundation for Basic Research (project no. 11-03-00168-a).

REFERENCES

1. Thinon, O., Diehl, F., Avenier, P., and Schuurman, Y., *Catal. Today*, 2008, vol. 137, p. 29.
2. Zonetti, P., Landers, R., and Cobo, A., *Appl. Surf. Sci.*, 2008, vol. 254, p. 6849.
3. Aouad, S., Abi-Aad, E., and Aboukai, A., *Appl. Catal., B,* 2009, vol. 88, p. 249.
4. Huang, L. and Xu, Y., *Appl. Catal., A*, 2001, vol. 205, p. 183.
5. Plyusnina, O.V., Emel'yanov, V.A., Baidina, I.A., et al., *Zh. Strukt. Khim.*, 2007, vol. 46, p. 114.
6. Sinitsyn, N.M., Kokunova, V.N., and Novitskii, G.G., *Zh. Neorg. Khim.,* 1985, vol. 30, p. 2870.
7. Il'in, M.A., Kuratieva, N.V., Kirichenko, O.A., et al., *Acta Crystallogr., Sect. E: Structure Reports Online,* 2005, vol. 61, no. 6, p. 126.
8. Herrera, J., Pope, S.J.A., Adams, H., et al., *Inorg. Chem.*, 2006, vol. 45, p. 3895.
9. Kuhlman, M.L. and Rauchfuss, T.B., *J. Am. Chem. Soc.*, 2003, vol. 125, p. 10084.
10. Davies, G.M., Pope, S.J., Adams, H., et al., *Inorg. Chem.*, 2005, vol. 44, p. 4656.
11. Kostin, G.A., Borodin, A.O., Shubin, Yu.V., et al., *Russ. J. Coord. Chem.*, 2009, vol. 35, p. 57.
12. Fletcher, J.M., Jenkins, I.L., and Lever, F.M., *J. Inorg. Nucl. Chem.,* 1955, vol. 1, p. 378.
13. Sheldrick, G.M., *Acta Crystallogr., Sect. A: Found. Crystallogr.*, 2008, vol. 64, p. 112.
14. Kostin, G., Borodin, A., Emel'yanov, V., et al., *J. Mol. Struct.*, 2007, vol. 837. P. 63.
15. Kostin, G.A., Borodin, A.O., and Kurat'eva, N.V., *Zh. Strukt. Khim.,* 2010, vol. 51, p. 598.
16. Pichkov, V.N., Zvyagintsev, O.E., and Sinitsyn, N.M., *Zh. Neorg. Khim.*, 1966, vol. 11, p. 2560.
17. Sinitsyn, N.M. and Kokunova, V.N., *Zh. Neorg. Khim.,* 1990, vol. 35, p. 3120.
18. ICDD/JCPDS PDF Database 2001. The International Centre for Diffraction Data Powder Diffraction File.
19. Massalski, T.B., *Binary Alloy Phase Diagrams*, Massalski T.B., Ed. Ohio: ASM International, 1990, with updates 1996.